

# Low-dose trametinib and Bcl-xL antagonist have a specific antitumor effect in KRAS-mutated colorectal cancer cells

MAKOTO KOYAMA<sup>1</sup>, MASATO KITAZAWA<sup>1</sup>, SATOSHI NAKAMURA<sup>1</sup>, TOMIO MATSUMURA<sup>2</sup>, SATORU MIYAZAKI<sup>1</sup>, YUSUKE MIYAGAWA<sup>1</sup>, FUTOSHI MURANAKA<sup>1</sup>, SHIGEO TOKUMARU<sup>1</sup>, MASAHIRO OKUMURA<sup>1</sup>, YUTA YAMAMOTO<sup>1</sup>, TAKEHITO EHARA<sup>1</sup>, NAO HONDO<sup>1</sup>, SHUGO TAKAHATA<sup>1</sup>, MICHIKO TAKEOKA<sup>1</sup>, SHIN-ICHI MIYAGAWA<sup>1</sup> and YUJI SOEJIMA<sup>1</sup>

<sup>1</sup>Department of Surgery, School of Medicine, Shinshu University; <sup>2</sup>Anaeropharma Science, Inc., Matsumoto, Nagano 390-8621, Japan

Received December 17, 2019; Accepted June 26, 2020

DOI: 10.3892/ijo.2020.5117

**Abstract.** KRAS-mutant colorectal cancer (CRC) is a highly malignant cancer with a poor prognosis, however specific therapies targeting KRAS mutations do not yet exist. Anti-epidermal growth factor receptor (EGFR) agents, including cetuximab and panitumumab, are effective for the treatment of certain patients with CRC. However, these anti-EGFR treatments have no effect on KRAS-mutant CRC. Therefore, new therapeutic strategies targeting KRAS-mutant CRC are urgently needed. To clarify the direct effect of KRAS gene mutations, the present study transduced mutant forms of the KRAS gene (G12D, G12V and G13D) into CACO-2 cells. A drug-screening system (Mix Culture assay) was then applied, revealing that the cells were most sensitive to the MEK inhibitor trametinib among tested drugs, Cetuximab, Panitumumab, Regorafenib, Vemurafenib, BEZ-235 and Palbociclib. Trametinib suppressed phosphorylated ERK (p-ERK) expression and inhibited the proliferation of KRAS-mutant CACO-2 cells. However, low-dose treatment with trametinib also increased the expression of the anti-apoptotic protein Bcl-xL in a dose-dependent manner, leading to drug resistance. To overcome the resistance of KRAS-mutant CRC to apoptosis, the combination of trametinib and the Bcl-xL antagonist ABT263 was assessed by *in vitro* and *in vivo* experiments. Compared with the effects of low-dose trametinib monotherapy, combination treatment with ABT263 had a synergistic effect on apoptosis in mutant KRAS transductants *in vitro*. Furthermore, *in vivo* combination therapy using low-dose trametinib and ABT263 against a KRAS-mutant (G12V) xenograft synergistically suppressed growth, with an increase in apoptosis compared with the effects of trametinib monotherapy. These data suggest that a

low dose of trametinib (10 nM), rather than the usual dose of 100 nM, in combination with ABT263 can overcome the resistance to apoptosis induced by Bcl-xL expression, which occurs concurrently with p-ERK suppression in KRAS-mutant cells. This strategy may represent a promising new approach for treating KRAS-mutant CRC.

## Introduction

Oncogenic KRAS mutations can be detected in approximately 40% of human colorectal cancers (CRCs) (1). Mutant KRAS remains activated because of impaired GTPase activity (2). Mutant KRAS has been demonstrated to contribute to the failure of anti-epidermal growth factor receptor (EGFR) antibodies, and it is associated with a poor prognosis in patients with CRC receiving adjuvant chemotherapy (3); however, the direct inhibition of mutant KRAS remains a pharmacological challenge. Previous studies revealed that a KRAS G12C-specific inhibitor (4-6) and a Src homology phosphotyrosine phosphatase 2 inhibitor can successfully inactivate mutant KRAS and inhibit tumorigenesis both *in vitro* and *in vivo* (7-9). However, to the best of our knowledge, clinically effective targeted agents for KRAS-mutant CRC do not exist.

Structural and functional analyses indicated that the MEK inhibitor trametinib can achieve superior efficacy in KRAS-driven tumors by inhibiting ERK1 and phosphorylated (p)-ERK1/2, as well as MEK1/2 phosphorylation and activation (10,11). MEK is a serine/threonine kinase that lies downstream of RAS in the RAS/MEK/ERK pathway, which regulates key cellular activities, including differentiation, proliferation and survival (12). The downstream position of MEK in this cascade makes it an attractive therapeutic target for patients whose tumors carry upstream gain-of-function mutations. Studies of multiple allosteric inhibitors of MEK in KRAS-mutant cancers have demonstrated targeted inhibition (13); however, their use has generally resulted in stable disease in early-stage clinical trials (14-17). In contrast to BRAF-mutant melanomas, which are highly sensitive to MEK inhibitors (18), this limited efficacy indicates that different mechanisms of inhibition are required for optimal antitumor activity against each phenotype.

**Correspondence to:** Dr Masato Kitazawa, Department of Surgery, School of Medicine, Shinshu University, 3-1-1 Matsumoto, Nagano 390-8621, Japan  
E-mail: kita118@shinshu-u.ac.jp

**Key words:** colorectal cancer, KRAS, Bcl-xL, trametinib, ABT263

MEK/ERK inhibitors have been demonstrated to induce the pro-apoptotic BH3-only protein BIM by suppressing ERK-mediated phosphorylation (19). BH3-only proteins appear to be critical for the response to targeted therapies, including EGFR and combined MEK/PI3K inhibitors (20,21). BIM, the most potent BH3-only protein, binds and neutralizes all anti-apoptotic B cell lymphoma 2 (Bcl2) proteins, such as Bcl-xL, whereas other BH3-only proteins (BID, BIK and NOXA) have greater restrictions (22). Therefore, the upregulation of BIM may offer the greatest potential to improve therapeutic efficacy. However, the induction of BIM proteins by MEK/ERK inhibition (23,24) is inhibited by the anti-apoptotic proteins Bcl2 and Bcl-xL, which are frequently overexpressed in solid tumors (25). In human CRC, Bcl-xL is significantly upregulated compared with its expression in normal mucosa and adenoma (26). In a study using mutant KRAS cell lines, mutant KRAS induced the upregulation of Bcl-xL protein expression (27).

We previously reported a proliferation screening assay system using green-fluorescent protein (GFP)-labeled transductants and fluorescence-activated cell sorting (FACS) (28). The present study modified this assay system to create the Mix Culture assay, which is an experimental system that can be used to screen for effective therapeutic targets in KRAS-mutant CRC cells. Through this screening, it was identified that a MEK inhibitor (trametinib) exerted a therapeutic effect on mutant KRAS (G12D, G12V, G13D)-transduced CACO-2 cells.

Trametinib suppressed the proliferation of KRAS-mutant cells by decreasing p-ERK expression, whereas Bcl-xL expression was increased. To overcome this resistance to apoptosis in KRAS mutants, the combination of trametinib and the Bcl-xL antagonist ABT263 was assessed both *in vitro* and *in vivo*. Trametinib was effective at low doses when used in combination with ABT263. Therefore, this therapy may also reduce the adverse effects of trametinib, such as liver injury. Trametinib and ABT263 combination therapy is expected to become a specific treatment for KRAS-mutant CRC.

## Materials and methods

**Cell culture.** Human CACO-2 cells were purchased from RIKEN BRC through the National Bio-Resource Project of the MEXT/AMED, Japan and maintained in DMEM (Gibco; Thermo Fisher Scientific, Inc.). Human SW48 cells were purchased from the American Type Culture Collection and maintained in RPMI-1640 with high glucose (FUJIFILM Wako Pure Chemicals Corporation). All cells were cultured in medium supplemented with 10% FBS (Biowest) and 1% penicillin/streptomycin at 37°C in 5% CO<sub>2</sub>.

**Antibodies and reagents.** The following antibodies were used: Monoclonal mouse FLAG (cat.no.014-22383; 1:1,000 for western blotting; FUJIFILM Wako Pure Chemicals Corporation); monoclonal rabbit ERK; cat. no. 4695; 1:1,000), monoclonal rabbit p-ERK (cat. no. 4376; 1:1,000), monoclonal mouse MEK1/2 (cat. no. 4694; 1:1,000), monoclonal rabbit p-MEK1/2 (cat. no. 9121; 1:1,000) and monoclonal rabbit Bcl-xL (cat. no. 2764; 1:1,000 for western blotting and 1:50 for immunostaining) all purchased from Cell Signaling Technology, Inc.; monoclonal mouse ribosomal s6 kinase (RSK; cat. no. sc-3933417; 1:200),

monoclonal mouse p-RSK (cat. no. sc-377526; 1:200), monoclonal mouse BIM (cat. no. sc-374358; 1:500), monoclonal mouse caspase-3 (cat. no. sc-7272; 1:500) and monoclonal mouse  $\beta$ -actin (cat. no. sc-47787; 1:2,000) purchased from Santa Cruz Biotechnology, Inc.; monoclonal mouse Bcl2 (cat. no. M0887; 1:1,000) purchased from Dako; Agilent Technologies, Inc.; and monoclonal rabbit Bcl2 (cat. no. ab32124; 1:100 for immunostaining) purchased from Abcam. The secondary antibodies polyclonal goat anti-mouse (cat.no.P0447; 1:5,000) IgG and polyclonal goat anti-rabbit (cat. no. P0448; 1:5,000) IgG conjugated with HRP were obtained from Dako; Agilent Technologies, Inc. Annexin V conjugated with APC and 7-aminoactinomycin D (7-AAD) was obtained from BioLegend, Inc. Cetuximab, panitumumab, trametinib and palbociclib were purchased from Merck KGaA, Takeda Pharmaceutical Company, Ltd., Cayman Chemical and LC Laboratories, respectively. Regorafenib, vemurafenib (cat. no. PLX4032), BEZ-235 and ABT263 were obtained from AdooQ Bioscience.

**Construction and retroviral transduction of the KRAS mutations.** Total mRNA from CACO-2 cells was extracted using NucleoSpin RNAPlus (Takara Bio, Inc.), and cDNA was synthesized using PrimeScript RT Master mix from the PrimeScript™ RT reagent kit (Takara Bio, Inc.). KRAS-4B carrying a C-terminal FLAG was amplified using PCR with PrimeSTAR® Max DNA Polymerase (Takara Bio, Inc.) using CACO2 cDNA as a template. The amplified KRAS-4B was inserted into the pMXs-IRES-GFP vector using the In-Fusion® HD Cloning kit (Takara Bio, Inc.) by the inverse PCR method. The thermocycling conditions were as follows: Denaturation at 98°C for 1 min, followed by 35 cycles of 98°C for 10 sec and 68°C for 20 sec for insert fragment, denaturation at 98°C for 1 min, followed by 35 cycles of 98°C for 10 sec and 68°C for 3 min for inverse vector. The following primers were used: KRAS-FLAG fragment forward: 5'-AGACTGCCGGATCCA ATGACTGAATATAAACTTGTGG-3', and reverse, 5'-GCG CCGGCCCTCGAGCTCGAGTCACTTGTCTCATCGTC CTTGTAATCGATCATAATTACACACTTTGT-3'; and pMXs-IRES-GFP vector forward #1, 5'-CTCAGAGGCCGG CGCGCCGCG-3', and reverse, 5'-TGGATCCGGCAGTCT AGAGG-3'. Next, pMXs-IRES-GFP vector carrying KRAS wild-type gene was used as a template to create vectors carrying the KRAS mutations (G12D, G12V, and G13D) with C-termined FLAG using the In-Fusion® HD Cloning kit by the inverse PCR method. The thermocycling conditions were the same as aforementioned and the following primers were used: G12D fragment forward, 5'-AAGTGTGTAATTATGGATGGCGTA GGCAAGAGTGCC-3'; G12V fragment forward, 5'-AAGTGT GTAATTATGGTTGGCGTAGGCAAGAGTGCC-3'; G13D fragment forward, 5'-AAGTGTGTAATTATGGGTGACGTA GGCAAGAGTGCC-3'; mutants (G12D, G12V and G13D) reverse, 5'-GTCCTTGTAATCGATCTCGAGTCACTTGTCTCATCGTC-3'; and pMXs-IRES-GFP vector forward #2, 5'-ATCGATTACAAGGACGATGACG-3', and reverse, 5'-CATAATTACACACTTTGTCTTTG-3'. Then, using the pMXs-IRES-GFP (KRAS wild, G12D, G12V and G13D) vectors as a template, pDON-5 Neo DNA vectors (Takara Bio, Inc.) carrying the KRAS wild-type and its mutations were constructed using the In-Fusion® HD Cloning kit by the inverse PCR method. The thermocycling conditions were the

same as aforementioned and the following primers were used: pDON-5 Neo fragment forward, 5'-CTCACGTGGGCCCCAAATGACTGAATATAAACTTG-3', and reverse, 5'-ACGTCGACGGATCCTTCACTTGTCTGTCATCGTCCTTG-3'; and pDON-5 Neo vector forward, 5'-AGGATCCGTCGACGTAAACGC-3' and reverse, 5'-TTGGGCCCCACGTGAGATCGAGC-3'. The DNA sequences of all constructs were confirmed by sequencing using a BigDye® Terminator v3.1 Cycle Sequencing kit (Thermo Fisher Scientific, Inc.) using sequence primers as follow: pMXs sequence, 5'-GACGGCATCGCAGCTTGGATACAC-3'; and pDON-5 Neo sequence, 5'-ATCTTGTTTCATTCTCAAGCCTC-3'. For retroviral transduction, 5 µg vectors were transfected into amphotropic packaging cells Phoenix-AMPHO (American Type Culture Collection) at 80% confluence on 60-mm cell dishes using 15 µl (1 µg/µl) PEI MAX (Polysciences, Inc.). The virus-containing supernatants were harvested after 24 and 48 h, and 50,000 CACO-2 and SW48 cells/well were infected with the retroviral particles on plates coated with RetroNectin (Takara Bio, Inc.). The transduction efficiency of pMXs-IRES-GFP vectors was confirmed using the GFP-positive ratio as measured using a flow cytometer and analyzed with Kaluza 2.1 software (Beckman Coulter, Inc.). And the cells from the 10th passage were used for the Mix Culture assay. Following transduction using pDON-5Neo DNA vectors, the transduced cells were selected via culture with G418 for 10 days. The transduction efficiency of pDON-5Neo DNA vectors was confirmed using western blotting.

**Cell proliferation assay.** CACO-2 cells were seeded at a density of  $1.0 \times 10^4/\text{cm}^2$  into 6-well plates and counted using the TC20™ Automated Cell Counter (Bio-Rad Laboratories, Inc.) after culture for 96 h. The Cell Counting Kit-8 (CCK8) assay was performed using a Cell Counting Kit-8 (CCK8) assay system (Dojindo Molecular Technologies, Inc.). Cells ( $5.0 \times 10^3/\text{well}$ ) were seeded into a 96-well tissue culture plate and incubated at 37°C. Following 24, 48, 72 and 96 h, CCK8 reagent (10 µl/well) was added and incubated for 3 h. Absorbance was measured using a plate reader at 450 nm. Cell growth was calculated as relative values from day 0 absorbance.

**Reverse transcription-quantitative PCR (RT-qPCR).** Total RNA was prepared from CACO-2 and SW48 cells, and mice xenograft tumors, using NucleoSpin RNA Plus (Takara Bio, Inc.) for RT. cDNA was synthesized using PrimeScript RT Master mix (Takara Bio, Inc.) at 37°C for 15 min and 85°C for 5 sec. qPCR was conducted using SYBER Premix Ex Taq™ II (Takara Bio, Inc.) and performed using a Mastercycler realplex<sup>2</sup> (Eppendorf). The thermocycling conditions were as follows: Denaturation at 95°C for 2 min, followed by 40 cycles of 95°C for 15 sec, 55°C for 15 sec, and 68°C for 20 sec. The relative expression level was calculated using the  $2^{-\Delta\Delta C_q}$  method (29). All data were normalized to the mRNA expression of TBP and presented as the fold increase relative to that in control cells. The following primers were used: TBP forward, 5'-GATCAGACAACAGCCTGCCAC-3' and reverse, 5'-TGGTGTCTGAATAGGCTGTGG-3'; Bcl-xL forward, 5'-GTGCGTGGAAGCGTAGACAAG-3' and reverse, 5'-GGCTGCTGCATTGTTCCCATAG-3'; and Bcl2 forward, 5'-GTGGCCTTCTTT

GAGTTCGGTG-3' and reverse, 5'-GAGTCTTCAGAGACAGCCAGGAG-3'.

**Protein sample preparation and western blotting.** CACO-2 and SW48 cells were lysed in RIPA lysis buffer (cat. no. sc-24948; Santa Cruz Biotechnology, Inc.) containing 1 mM PMSF on ice for 30 min. The lysates were separated by centrifugation at  $10,000 \times g$  for 10 min at 4°C and the resultant supernatant was collected as the total cell lysate. Protein was quantified using a Pierce BCA Protein assay kit (Thermo Fisher Scientific, Inc.) and 10–12.5 µg protein was separated using 15% SDS-PAGE and then electroblotted onto a PVDF membrane. The membrane was blocked with Tris-buffered saline containing 5% non-fat dry milk and 1% Tween-20 for 1 h at room temperature and then probed using the primary antibodies at 4°C overnight. The membrane was then incubated with horseradish peroxidase-conjugated secondary antibody for 1 h at 4°C, which was detected by enhanced chemiluminescence using Immobilon Western HRP (Amersham ECL Prime Western Blotting Detection Reagent; Cytiva). The density of the target protein measured using Image Lab Software version 6.0.1 (Bio-Rad Laboratories, Inc.) was divided by the density of each β-actin to obtain the actual density. Relative densities of various treatments were calculated with the actual density of wild type as 1.

**Annexin V/7-AAD assay.** CACO-2 cells were incubated with 50 nM trametinib and/or 1 µM ABT263 for 48 h at 37°C. Trypsin was added to detach adherent cells, which were then combined with floating cells. Cells were incubated with Annexin V conjugated with APC and 7-AAD for 15 min at room temperature (25°C). The labeled cell populations were quantitated by flow cytometry using Kaluza Analysis Software v2.1 (Beckman Coulter, Inc.).

**Mix Culture assay.** In order to screen for effective therapeutic targets stably and reliably, an *in vitro* Mix Culture assay experimental system was developed using the pMX-IRES-GFP vector and FACS. For this assay, wild-type and mutant KRAS genes (G12D, G12V and G13D) inserted into the pMX-IRES-GFP vector were transduced into CACO-2 cells retrovirally. A high gene transduction efficiency of  $\geq 90\%$ , as determined by the GFP-positive rate (%) measured using FACS, was obtained (Fig. 1A). Parental cells (GFP-negative) and gene-transduced cells (GFP-positive) were mixed at an ideal 1:1 ratio, as shown in Fig. 1B. On the first day, the mixed cells were seeded at 20% confluency into a 12-well plate and cultured for 12 days with molecular targeted agents. They were then passaged at a 5:1 ratio before reaching confluence. On day 12, the cells were harvested and stained with 7-AAD. 7-AAD-negative populations representing viable cells were gated, and the GFP-positive ratio of these populations was determined using FACS. The relative proliferation ratio (RPR) was calculated using the day 0 GFP-positive rate (%), A and the day 12 GFP-positive rate (%), B.  $RPR = B(100-A)/A(100-B)$ . The outline of this experimental system, and an experimental example are shown. A low RPR indicated that the GFP-positive cell population was sensitive to the drug, whereas a high RPR indicated drug resistance (Fig. 1B).



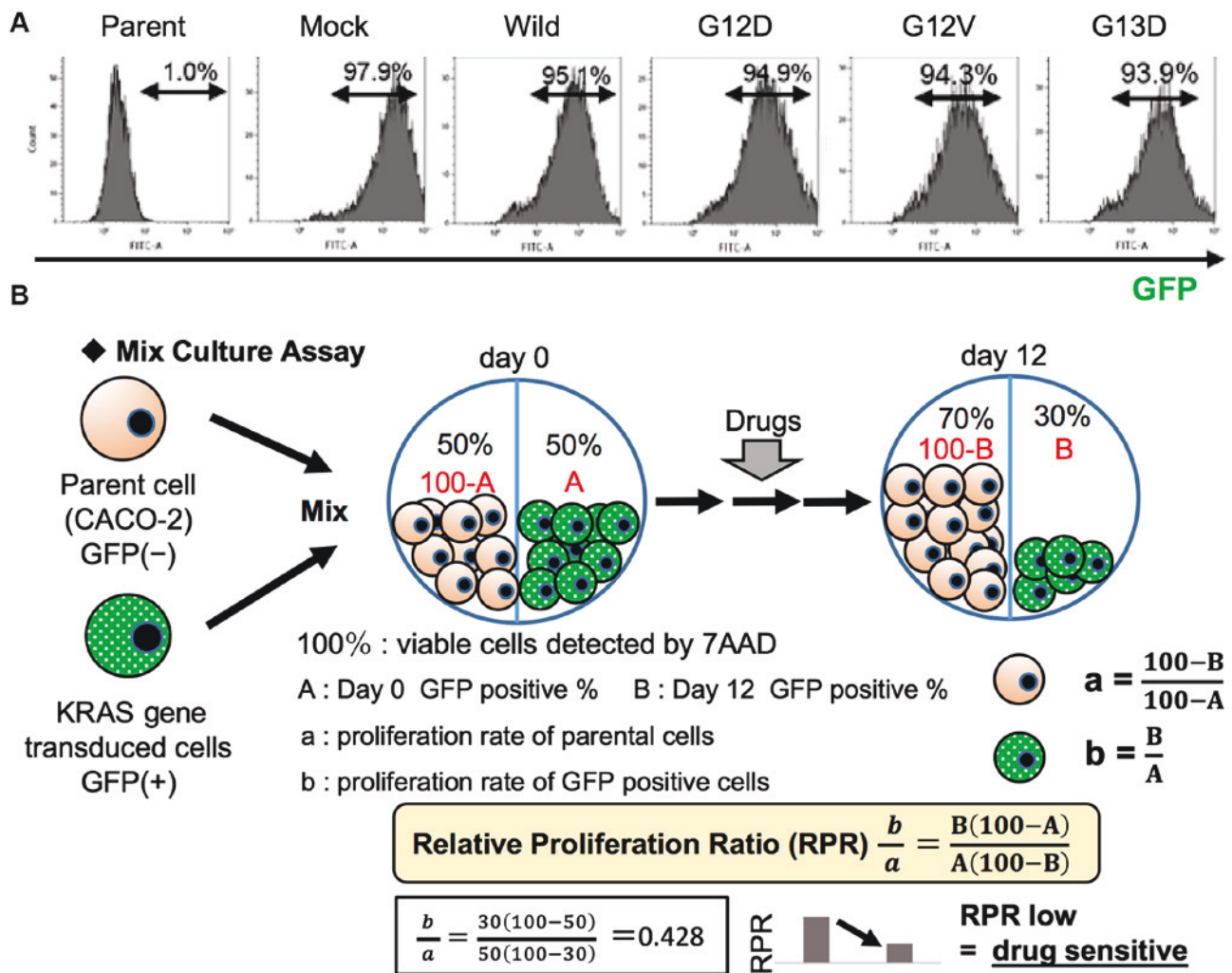


Figure 1. Mix Culture Assay system for drug screening. Wild and mutant KRAS genes in pMX-IRES-GFP vectors were retrovirally transduced into CACO-2 cells. (A) The transfection efficiency was confirmed by the GFP-positive rate (%) via fluorescence-activated cell sorting. (B) Schematic of the Mix Culture Assay. The RPR was calculated using the day 0 and day 12 GFP-positive rates (%). wild, wild-type; GFP, green-fluorescent protein; p-, phosphorylated; 7-AAD, 7-aminoactinomycin D; RPR, relative proliferation ratio.

**In vivo xenograft experiments.** All animal experiments were carried out following the national standard of the care and use of laboratory animals, and the study was approved by the Animal Research Committee of Shinshu University (Matsumoto, Japan; approval no. 019046). A total of 30 mice were used in the present study. Mice were kept in a pathogen-free room under standard conditions with a controlled temperature ( $23 \pm 3^\circ\text{C}$ ), humidity and a 12-h light/dark cycle. Mice had free access to water and food. The male 6-8-week-old BALB/c nude mice (weight, 24-27 g) were purchased from CLEA Japan, Inc. Mice were kept in a pathogen-free room with a 12-h light/dark cycle and free access to water and food. For tumorigenesis assays, xenograft tumors were generated via the subcutaneous injection of CACO-2 cells ( $5 \times 10^6$ ) stably expressing wild-type or G12V mutant KRAS in 200  $\mu\text{l}$  solution [50% Hank's Balanced Salt Solution (FUJIFILM Wako Pure Chemicals Corporation) + 50% Matrigel (Corning, Inc.)] into the flanks of 6-8-week-old male BALB/c nude mice. For the reagent experiment, vehicle (12.5% Cremophor, 12.5% ethanol, 75%), trametinib (0.1 mg/kg) and/or ABT-263 (5 mg/kg) were orally administered once daily for 10 consecutive days to mice (n=4

per group) that had been subcutaneously injected with CACO-2 cells expressing the KRAS G12V gene. The tumor volume was measured twice weekly according to the following formula: Volume ( $\text{mm}^3$ ) =  $0.5 \times \text{width}^2$  (mm)  $\times$  length (mm). All mice were sacrificed by cervical dislocation under 3% sevoflurane anesthesia on day 20 and were weighed.

**Immunohistochemistry and TUNEL staining.** The resected xenograft tumors were fixed in 4% paraformaldehyde overnight at RT and embedded in paraffin, and then tissue sections (5- $\mu\text{m}$ ) were prepared and stained with a primary antibodies against Bcl-xL or Bcl2. Antigen retrieval was performed by boiling the sections at  $98^\circ\text{C}$  for 45 min in 0.05 M citric acid buffer (pH 6.0) for Bcl-xL and 1 mM EDTA2Na solution (pH 9.0) for Bcl2. The slides were then subjected to endogenous peroxidase blocking with 3%  $\text{H}_2\text{O}_2$ . The primary antibodies were added to the slides, which were incubated overnight at  $4^\circ\text{C}$ . Subsequently, the slides were visualized using Histofine Simplestain Max PO kit (cat. no. 414142F; Nichirei Bioscience, Inc) for 1 h at room temperature. HRP-conjugated streptavidin was used to attach peroxidase to the antibodies,

and DAB chromogen was used for visualization. Then, hematoxylin was used for nuclear counterstaining for 30-60 sec at room temperature.

The *in situ* detection of DNA fragmentation in the tumor tissues was performed using TUNEL staining with an *in situ* apoptosis detection kit (cat. no. MK500; Takara Bio, Inc.). Deparaffinized sections (5- $\mu$ m) were treated with 10  $\mu$ g/ml proteinase K and left at room temperature for 15 min. The endogenous peroxidase was inactivated by applying 3% H<sub>2</sub>O<sub>2</sub> for 5 min. The slides were treated with 50  $\mu$ l labeling reaction mixture (consisting of 5  $\mu$ l TdT enzyme + 45  $\mu$ l labeling safe buffer) and incubated at 37°C for 60-90 min. Then, the slides were incubated with 70  $\mu$ l anti-FITC HRP conjugate at 37°C for 30 min. The slides were stained with 3% methyl green for 1-2 min at room temperature to visualize the nuclei. The numbers of TUNEL-positive cells were counted in five random high-power fields using a light microscope (magnifications, x20 and x400; Olympus Corporation). CellSense Standard (v1.7.1; Olympus Corporation) was used to observe the images. The obtained images were analyzed using ImageJ analysis software v1.50i (National Institutes of Health) to calculate the number of TUNEL-positive cells.

**Statistical analysis.** Data are expressed as the mean  $\pm$  standard deviation of 4-5 experiments for each assay. Statistical analysis was performed using JMP® v14.2 (SAS Institute Inc.) for analysis. Statistical significance was evaluated using an unpaired Student's t-test or one-way ANOVA followed by Bonferroni's correction.  $P < 0.05$  was considered to indicate a statistically significant difference.

## Results

**Mutant KRAS promotes cell proliferation via the upregulation of ERK phosphorylation.** To investigate the effects of oncogenic mutations in KRAS in CRC cells, wild-type and mutant KRAS genes (G12D, G12V and G13D) carrying a C-terminal FLAG were inserted into pDON-5Neo DNA vectors, which were retrovirally transduced into CACO-2 and SW48 human CRC cells expressing wild-type KRAS. Transduction was confirmed using an anti-FLAG antibody (Fig. 2A). The effect of KRAS gene mutation on cell proliferation were then examined. Mutant KRAS-transduced CACO-2 cells exhibited a significantly higher rate of proliferation compared with cells transduced with wild-type KRAS. This data was supported by CCK8 assay (Fig. 2B). The RAS/MEK/ERK signaling pathway is known to act downstream of the KRAS gene and regulate key cellular activities including differentiation, proliferation and survival. Therefore, p-MEK, p-ERK and p-RSK expression was examined using western blotting, and the ratios of p-protein/total protein were significantly higher in all mutant KRAS cells compared with in wild-type cells (Figs. 2C and S1A). Subsequently, other pathways associated with the RAS/MEK/ERK pathway were examined using the Mix Culture assay system.

**Mutant KRAS upregulates the anti-apoptotic markers Bcl-xL and Bcl2.** MEK inhibitors are known to induce apoptosis via the pro-apoptotic protein, Bim, and it has been reported that when Bim-mediated apoptosis is induced by MEK inhibitors, Bcl-xL

and Bcl2 are also induced, which contributes to the resistance of MEK inhibitors (25). Therefore, the present study examined the expression of Bcl-xL and Bcl2 in KRAS-transduced CACO-2 and SW48 cells to evaluate whether the expression of these molecules differed in cells with mutant KRAS. The mRNA levels of Bcl-xL were significantly higher in all mutant KRAS-transduced CACO-2 and SW48 cells compared with the wild-type cells. Bcl2 was significantly higher only in mutant KRAS-transfected CACO-2 cells but not in SW48 cells (Fig. 2D). Previously it was reported that KRAS mutations affect Bcl-xL expression more strongly than Bcl2 (27). Therefore, it can be hypothesized that KRAS strongly affects Bcl-xL but not Bcl2 in SW48 cells. The protein expression of Bcl-xL was also significantly upregulated in all KRAS-mutant cells, except for in G13D SW48 cells. The expression of Bcl2 protein was not higher in the KRAS mutants compared with the wild-type (Figs. 2E and S1B). These results suggested that Bcl-xL may be a therapeutic target in KRAS-mutant CRCs.

**Mix Culture assay can detect MEK inhibitor (trametinib) sensitivity in KRAS gene-mutant CACO-2 cells with suppressed ERK phosphorylation.** Using a Mix Culture assay system, the drug sensitivities of KRAS-transduced cells to several drugs were examined. EGFR inhibitors (cetuximab and panitumumab) dose-dependently induced a significantly high RPR in KRAS-mutant CACO-2 cells, indicating that KRAS mutations (G12D, G12V and G13D) led to resistance to EGFR inhibitors (Fig. 3A). A multi-kinase inhibitor (regorafenib), BRAF inhibitor (vemurafenib), PIK3CA inhibitor (BEZ234) and CDK4/6 inhibitor (palbociclib) did not change the RPR. By contrast, a MEK inhibitor (trametinib) reduced the RPR in KRAS-mutant cells in a dose-dependent manner significantly in G12D and G12V (Fig. 3A). Treatment with trametinib (1-10 nM) suppressed ERK phosphorylation both in KRAS wild type and mutant cells in a dose-dependent manner, however the concentration of trametinib that suppressed p-ERK level was different between the KRAS mutants and wild type (Figs. 3B and S2).

**Combined treatment with ABT263 and low-dose trametinib effectively induces apoptosis in mutant KRAS-transduced CACO-2 cells.** According to Zaanen *et al* (27), the treatment of HCT116 and SW620 cells with the MEK inhibitor GDC-0623 at clinically relevant doses has no effect on Bcl-xL expression; however, inhibition of Bcl-xL synergistically enhances GDC-0623-induced apoptosis. To investigate the influence of trametinib on apoptosis in wild-type and mutant KRAS (G12V)-transduced CACO-2 cells, trametinib (100 nM) was administered according to the methodology described by Yamaguchi *et al* (10). As a result, 100 nM trametinib increased cleaved caspase 3 expression, with a significant dose-dependent increase in BIM, expression observed in mutant cells. The increase in BIM was also observed in wild-type cells. (Figs. 4A-a and S3A). A similar increase in BIM expression was observed; however, cleaved caspase 3 expression was hardly detected in wild-type cells (Figs. 4A-a and S3A). Trametinib (100 nM) did not alter Bcl-xL or Bcl2 protein levels in the mutant cells (Figs. 4A-b and S3B), similar to the results reported by Zaanen *et al* (27). Next, the effect of the combined treatment of ABT263 and trametinib was

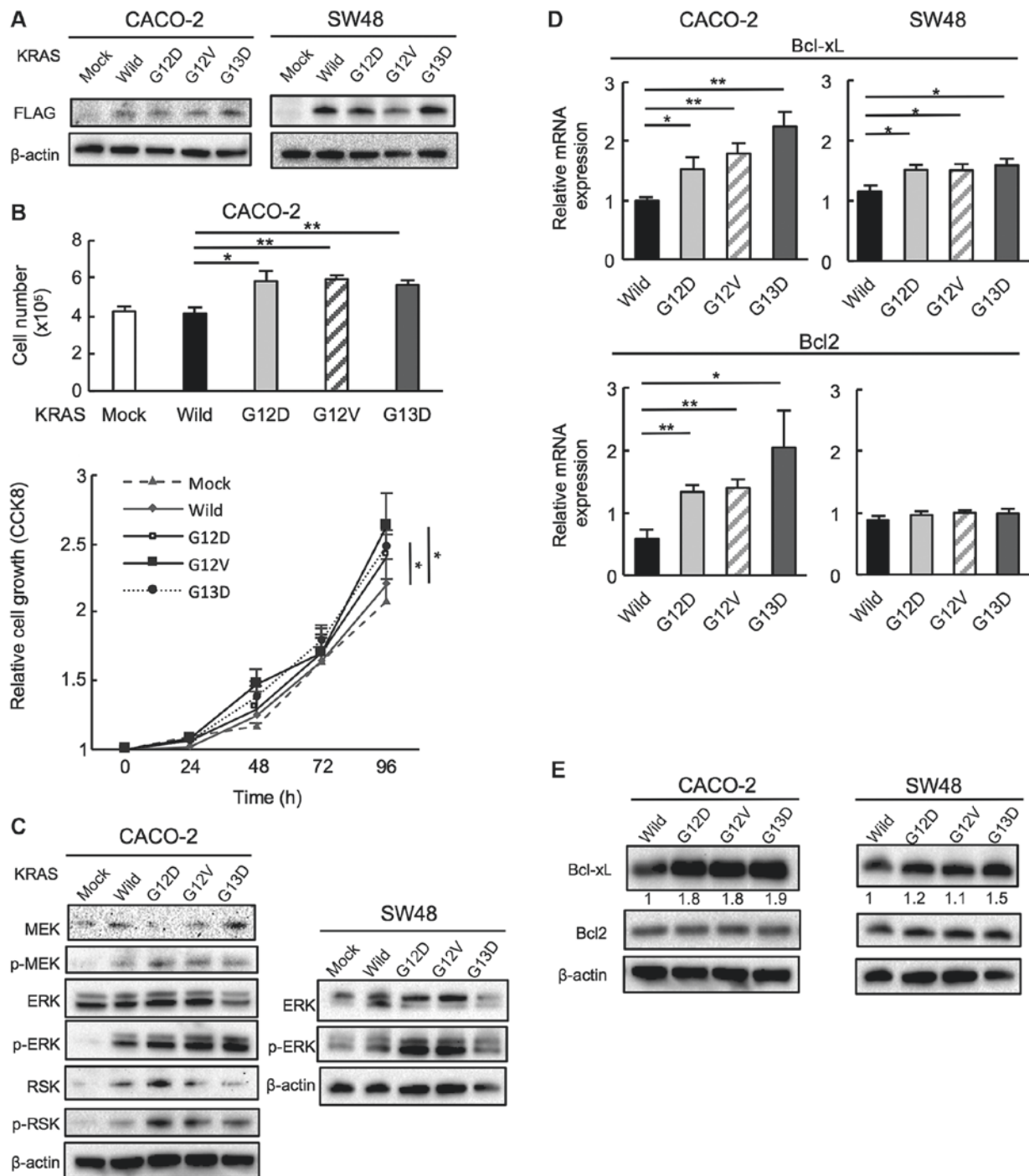


Figure 2. Mutant KRAS promotes CACO-2 and SW48 cell proliferation via the upregulation of ERK phosphorylation. (A) The transduction of KRAS wild and mutant (G12D, G12V and G13D) genes was confirmed using western blotting with a FLAG-specific antibody. (B) Proliferation was evaluated by counting the cell number at 96 h and use of CCK8 at 24, 48, 72 and 96 h after cell seeding. *n*=5. \**P*<0.05, \*\**P*<0.01. (C) MEK, ERK and RSK phosphorylation in CACO-2 cells and ERK phosphorylation in SW48 cell was examined using western blotting. Mutant KRAS upregulates anti-apoptotic Bcl-xL and Bcl2 expression. The expression levels of Bcl-xL and Bcl2 in cells transduced with wild and mutant KRAS (G12D, G12V and G13D) were examined by (D) reverse transcription-quantitative PCR and (E) western blotting. *n*=5. \**P*<0.05, \*\**P*<0.01. Wild, wild-type; CCK8, Cell Counting Kit-8; p-, phosphorylated.

examined in mutant KRAS transduced cells. Combined with ABT263 (1  $\mu$ M), trametinib significantly increased cleaved caspase 3 expression in a dose-dependent manner at with a large increase in BIM protein levels also observed indicating the dose-dependent increase in apoptosis. Trametinib (100 nM) alone demonstrated a sufficient effect of suppressing p-ERK expression, and the effect was similar when ABT263 was used in combination. The effect of combination treatment

on cleaved caspase 3 was more significant at trametinib doses of 50 or 100 nM compared with trametinib alone (Figs. 4A-c and S3C).

Using our Mix Culture assay, the effects of low-dose trametinib on anti-apoptotic protein expression in KRAS-mutant CACO-2 cells were then investigated. Notably, Bcl-xL expression was increased in a dose-dependent manner by low doses of trametinib (0-10 nM) in G12D and G12V



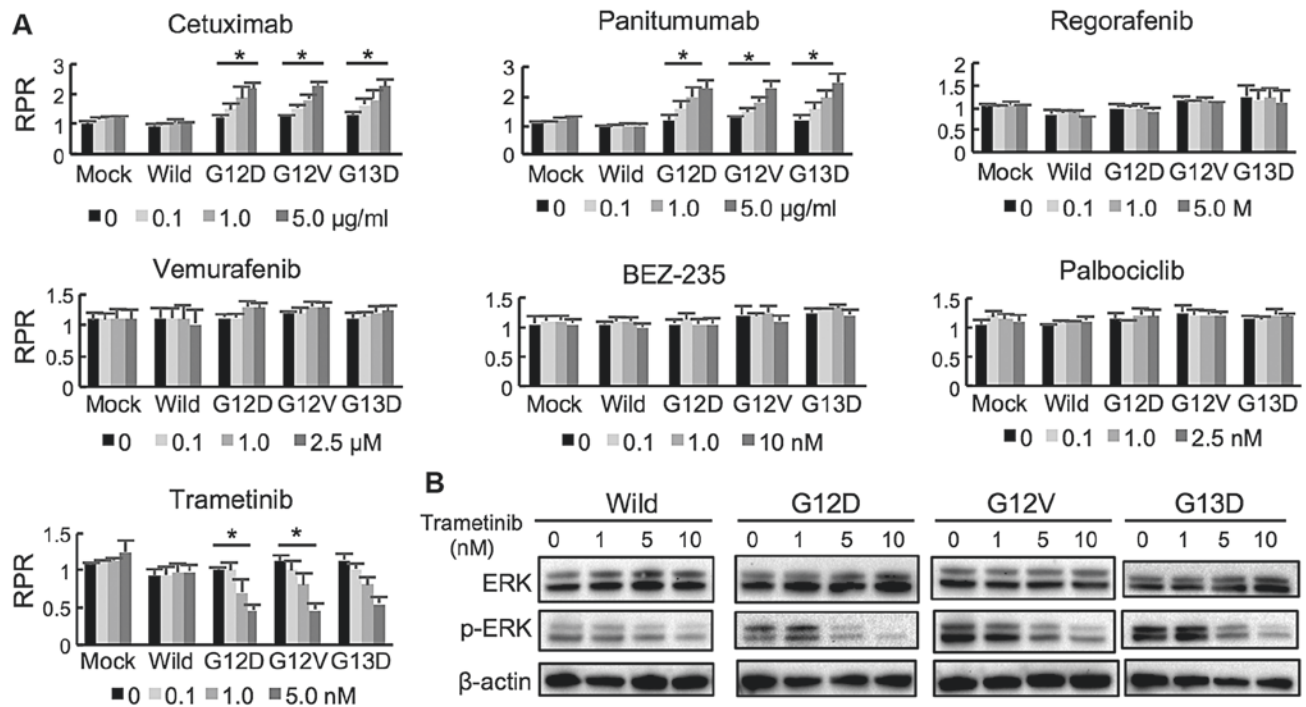


Figure 3. Mix culture assay detects sensitivity to a MEK inhibitor (trametinib) in KRAS gene-mutant CACO-2 cells with suppressed ERK phosphorylation. (A) Wild-type and mutant KRAS CACO-2 cells were treated with the indicated doses of an epidermal growth factor inhibitor (Cetuximab and Panitumumab), multi-kinase inhibitor (Regorafenib), BRAF inhibitor (Vemurafenib), PIK3CA inhibitor (BEZ-235), CDK4/6 inhibitor (Palbociclib), or MEK inhibitor (Trametinib).  $n=4$  each,  $^*P<0.05$ . (B) Phosphorylation of ERK following trametinib treatment was detected using western blotting. RPR, relative proliferation ratio; Wild, wild-type; p-, phosphorylated.

mutants (Figs. 4B and S4). Accordingly, it was hypothesized that ABT263 can suppress Bcl-xL function and induce apoptosis when combined with low-dose (10 nM) trametinib to a similar extent as high dose (100 nM) trametinib. In fact, combined treatment with ABT263 and low-dose trametinib significantly enhanced the cleavage of caspase 3 in KRAS G12V cells compared with in wild-type cells, and this combination therapy induced apoptosis in cells carrying other KRAS variants (G12D and G13D) in the same manner (Figs. 4C and S5A).

These apoptosis data were supported by results of the FACS assay. These results demonstrated that apoptosis was enhanced by combination therapy in cells carrying KRAS variants, whereas this effect was not observed in wild-type cells (Fig. S5B and C). Furthermore, the Mix Culture assay data supported these results, indicating that combined low-dose trametinib (1 nM) and ABT263 (5  $\mu\text{M}$ ) therapy significantly suppressed the RPR in G12D and G12V mutant KRAS-transduced cells compared with cells treated with trametinib, a result that was not seen in wild-type cells (Fig. 4D). Thus, the effectiveness of combination therapy consisting of low-dose trametinib and ABT263 was for facilitating apoptosis and suppressing the proliferation of G12D and G12V KRAS-mutant CACO-2 cells was confirmed.

**KRAS mutation (G12V) is associated with tumorigenesis by upregulating Bcl-xL and Bcl2 expression in vivo.** The present study examined the effects of KRAS mutation on tumorigenicity *in vivo* using CACO-2 cells transduced with wild-type and mutant KRAS (G12V). As presented in Fig. 5A, the tumor volume of mutant KRAS-bearing murine subcutaneous xenografts was significantly larger than that of mice bearing

wild-type xenografts on day 21. The tumor weight was also significantly larger for the KRAS-mutant xenografts (Fig. 5B). Bcl-xL and Bcl2 mRNA expression was significantly higher in KRAS-mutant xenografts compared with in wild-type xenografts (Fig. 5C). Furthermore, immunohistochemistry revealed that Bcl-xL expression was higher in KRAS-mutant xenografts, whereas Bcl2 expression was not different between wild-type and mutant xenografts (Fig. 5D). These results suggest that the KRAS G12V mutation promotes tumorigenesis by increasing Bcl-xL expression *in vivo*.

**Combined treatment with low-dose trametinib and ABT263 effectively inhibits tumor growth and induces apoptosis in murine xenografts of mutant KRAS (G12V)-transduced CACO-2 cells.** Low-dose trametinib (0.1 mg/kg), rather than the usual dose of 1-3 mg/kg (10,11), was used in this experiment based on the results of the *in vitro* experiments to efficiently and effectively suppress tumor progression.

Trametinib and ABT263 monotherapy suppressed tumor growth, but combined treatment with both agents significantly reduced tumor growth on day 20 compared with the individual treatments alone (Fig. 6A). The fluctuation in body weight was within 10% in all mice throughout the experiments, and the weights of the mice on day 20 ranged between 26-28 g (Fig. 6A). The combined treatment resulted in a significantly smaller tumor weight (Fig. 6B) and an increase in cell death, as visualized using TUNEL staining (Fig. 6C), compared with the individual treatments on day 20. Accordingly, combination therapy with low-dose trametinib and ABT263 was found to be more effective against mutant KRAS (G12V)-transduced tumors than trametinib or ABT263 alone *in vivo*. A schematic

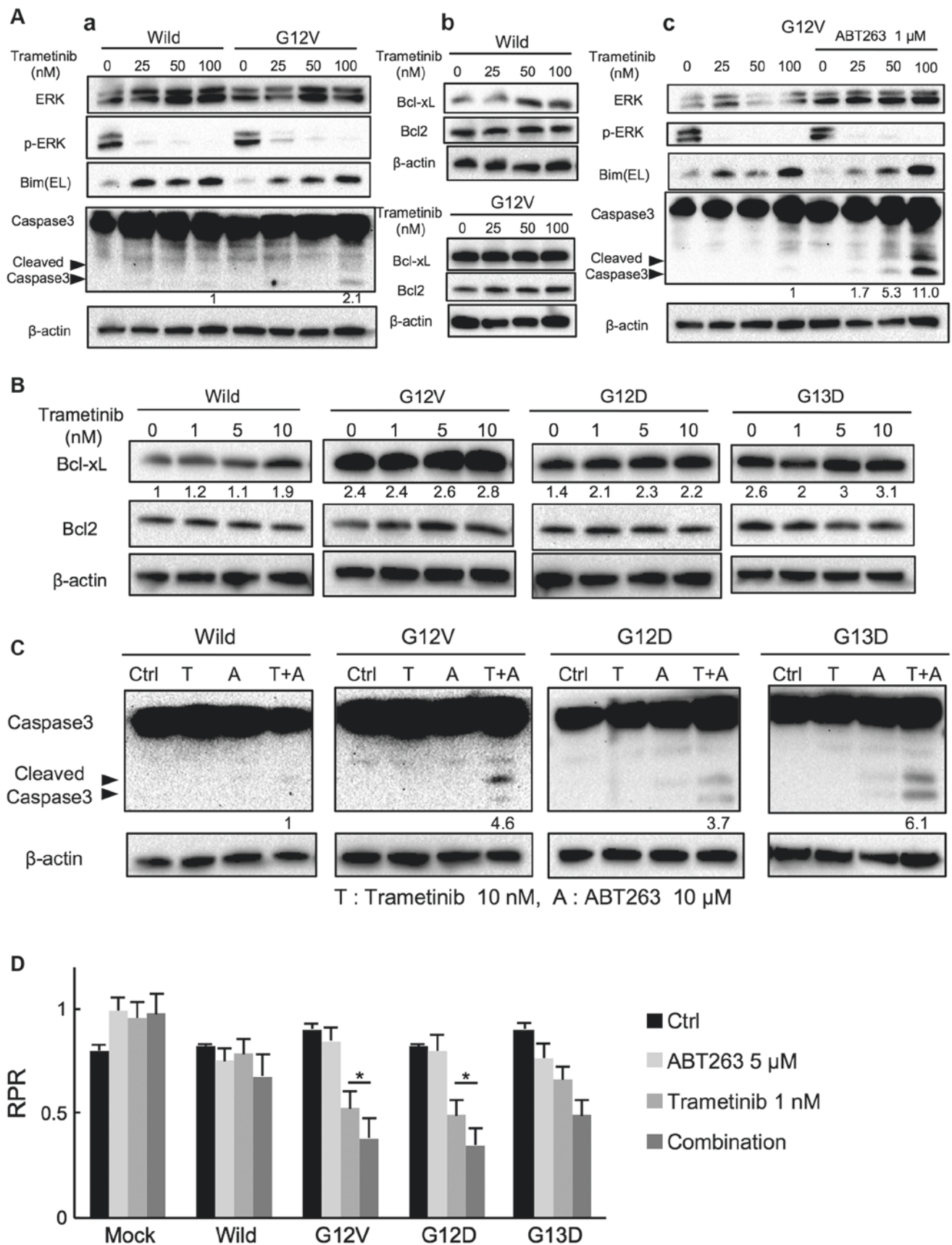


Figure 4. Combined treatment with ABT263 and low-dose trametinib effectively induces apoptosis in mutant KRAS-transduced CACO-2 cells. (A) Trametinib decreased p-ERK and increased BIM expression. Apoptosis as detected by cleaved caspase 3 expression (A-a) and Bcl-xL and Bcl2 expression following trametinib (0-100 nM) treatment was evaluated using western blotting (A-b). Apoptosis induced by the combination of trametinib (100 nM) and ABT263 (1  $\mu$ M) was evaluated by detecting caspase 3 expression using western blotting (A-c). (B) Bcl-xL and Bcl2 expression following low-dose trametinib treatment (0-10 nM) was evaluated using western blotting. (C) Effects of combined low-dose trametinib and ABT263 treatment were evaluated by assessing caspase 3 levels using western blotting. (D) Effects of low-dose trametinib and/or ABT263 on proliferation were confirmed using the Mix Culture Assay. n=4. \*P<0.05. p-, phosphorylated; wild, wild-type; RPR, relative proliferation ratio; Ctrl, control; EL, extra long.



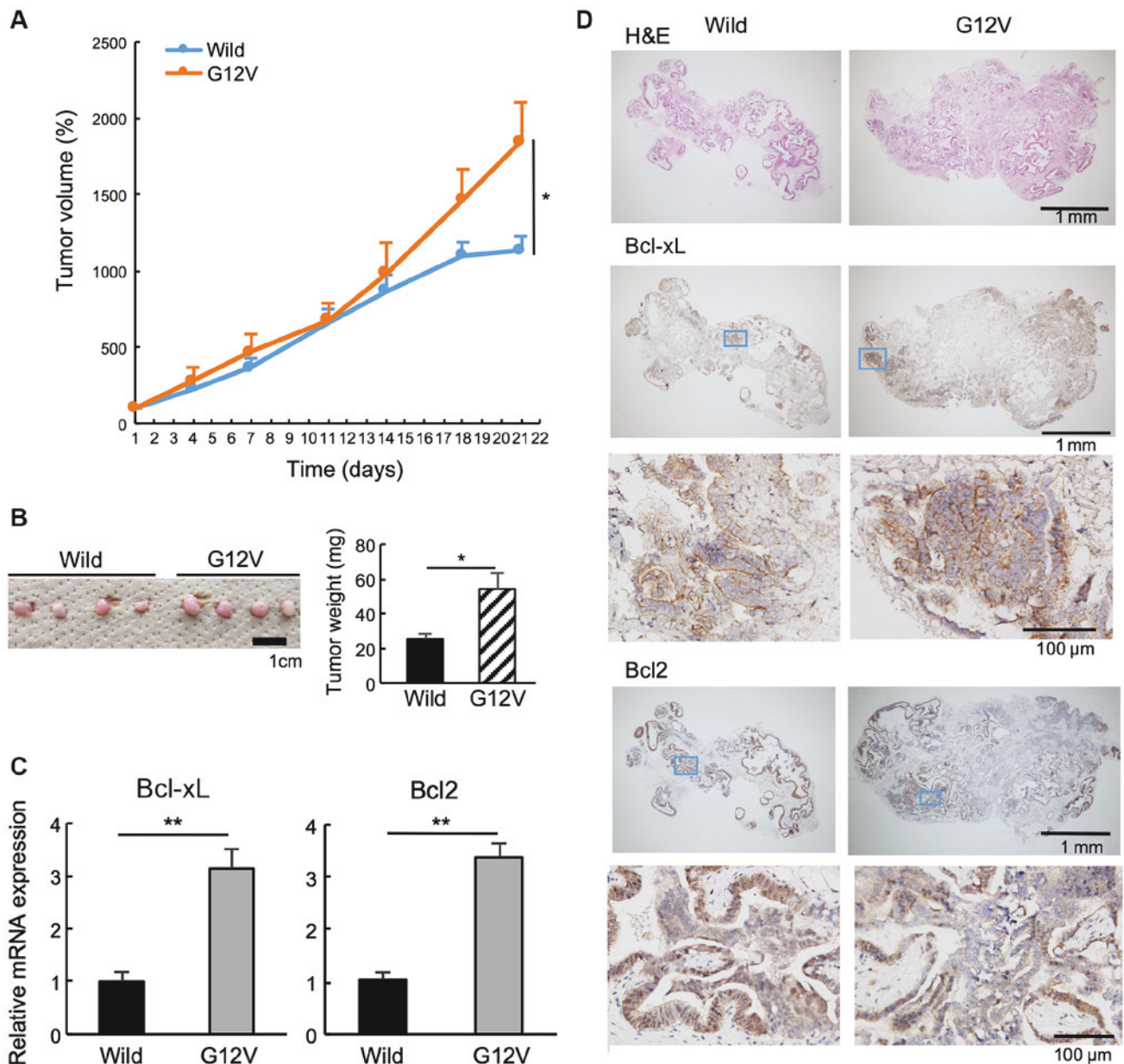


Figure 5. Mutant KRAS promotes tumorigenesis by upregulating Bcl-xL and Bcl2 expression *in vivo*. Wild and mutant (G12V) KRAS-expressing CACO-2 cells were subcutaneously inoculated in nude mice. The (A) tumor volume and (B) weight on day 21 of wild and mutant murine xenografts are presented. n=4 each. (C) The expression of Bcl-xL and Bcl2 in the xenografts was detected via reverse transcription-quantitative PCR. n=4. \*P 0.05, \*\*P<0.01. (D) Immunohistochemistry of wild and mutant xenografts was compared on day 21. The inset is the magnified image. wild, wild-type.

of the mechanism by which trametinib and ABT263 combination therapy is considered to induce apoptosis is shown in Fig. 6D. KRAS mutation results in p-ERK and Bcl-xL overexpression. Trametinib suppresses p-ERK expression, while increases Bcl-xL expression and may induce resistance to apoptosis. Therefore, ABT263 combined with trametinib effectively induces apoptosis probably via increased BIM expression in KRAS-mutant CRC.

## Discussion

In basic research, numerous reports have demonstrated the effect of MEK inhibitors against mutant KRAS cancers (10,11); however, to the best of our knowledge, no clinical trials have demonstrated the efficacy of MEK inhibitors. Our drug

screening system, the Mix Culture assay, suggested that the MEK inhibitor trametinib, among several tested agents, had a therapeutic effect on KRAS-mutant CACO-2 cells. Thus, experiments were performed to identify the therapeutic target(s) of trametinib in KRAS-mutant CRC. It was revealed that the low-dose trametinib inhibited tumor cell proliferation and suppressed p-ERK expression, while simultaneously increasing Bcl-xL protein expression in mutant KRAS transductants. The combination of low-dose trametinib and the anti-Bcl-xL/Bcl2 agent ABT263 increased the efficacy of tumor suppression. The efficacy of this combination therapy against KRAS transductants was validated using both *in vitro* and *in vivo* xenograft models.

Anti-EGFR agents are effective for the treatment of certain patients with CRC (30-32); however, anti-EGFR treatments are

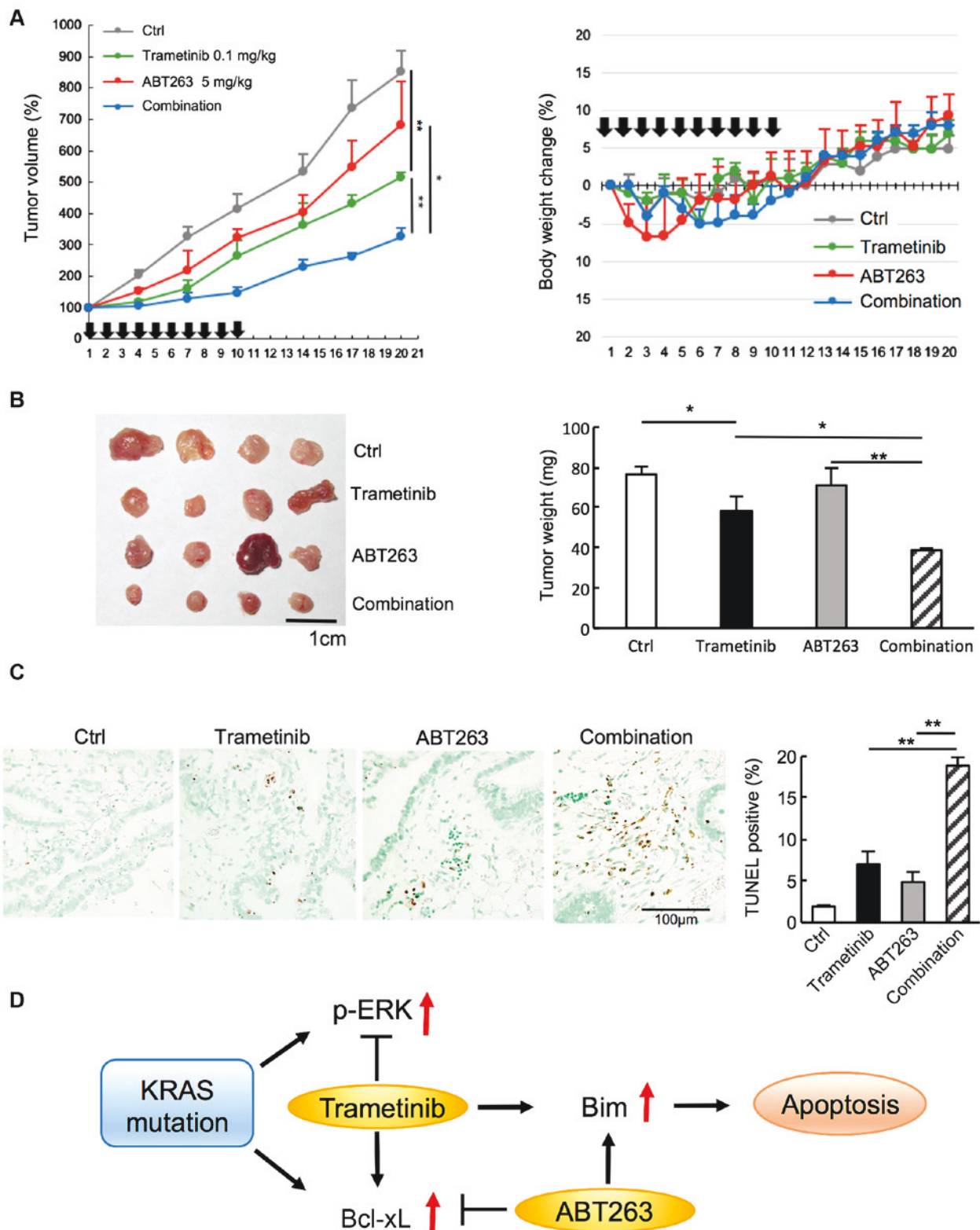


Figure 6. Combined treatment with low-dose trametinib and ABT263 effectively inhibits tumor growth and induces apoptosis of murine subcutaneous mutant KRAS (G12V)-transduced CACO-2 cells. KRAS wild-type and G12V-mutated CACO-2 cells were subcutaneously inoculated into nude mice and the mice were treated daily with trametinib and/or ABT263 for 10 days. The (A) tumor volume and body weight, and the (B) tumor weight on day 20 of the KRAS-mutated murine xenografts. The arrows indicate the days that reagents were administered.  $n=4$  for each. (C) Cell death was visualized in five random fields using TUNEL staining on day 20. (D) The mechanism of how trametinib and ABT263 combined therapy induces apoptosis in mutant KRAS-transduced CRC cells. \* $P<0.05$ , \*\* $P<0.01$ . p-, phosphorylated; Ctrl, control.

ineffective in patients with KRAS-mutant CRC (33,34). As part of the search for new therapeutic targets in KRAS-mutant CRC, numerous reports have used KRAS-mutant cell lines,

such as DLD-1, HCT116 and SW620 (25,27,35). To examine the effects of KRAS gene mutation on several signaling pathways, the present study introduced KRAS gene mutations (G12D,

G12V and G13D) into CACO-2 and SW48 cells expressing wild-type RAS (KRAS, HRAS, NRAS) (36). Mutant KRAS transductants exhibited increased proliferation and p-ERK protein overexpression due to RAS/MEK/ERK activation.

We previously reported a FACS-based assay system using GFP-labeled transduced cells and parental cells (28). We have since modified this system and developed a new drug screening assay named the Mix Culture Assay, in which sensitivity/resistance is evaluated using the RPR as an index. Because parental cells were mixed as an internal control and the ratio of transfectants to parental cells was evaluated using FACS as the GFP-positive rate, this assay is considered to be relatively stable and reproducible compared with conventional set-ups. Our assay also avoids the risk of selecting champion clones, which limits the reliability of stable clone assays. The present study identified the sensitivity of KRAS-mutant transductants to the MEK inhibitor trametinib using this system.

Trametinib is reportedly more effective against KRAS-mutant cell lines (HCT-116 and SW620) than against wild-type cells (10,11). The present study identified that commonly used doses of trametinib (25-100 nM) can potently downregulate p-ERK and upregulate BIM expression in KRAS transductants. BIM is the most potent pro-apoptotic BH3-only protein given its ability to neutralize all anti-apoptotic Bcl2 family proteins (22). The activity of upregulated BIM was detected by the presence of cleaved caspase 3 in KRAS-mutant cells in the current study.

Despite the induction of BIM, mutant KRAS transductants exhibited resistance to the MEK inhibitor trametinib. Zaanani *et al* (27) reported that resistance to MEK inhibitors in DLD-1 cells (KRAS mutant) is partly attributable to the upregulation of Bcl-xL, indicating that MEK/ERK inhibition and related BIM induction are insufficient to overcome mutant KRAS-mediated apoptosis resistance. Trametinib (25-100 nM) could not suppress the expression of Bcl-xL in the G12V transductants. These data may underlie the limited efficacy of MEK inhibitors against KRAS-mutant tumors even when complete suppression of the RAS/MEK/ERK signaling pathway has been achieved. Although the mechanisms by which KRAS activation can suppress apoptosis are poorly understood, it was identified that Bcl-xL mRNA and protein expression was upregulated in all KRAS-mutant cells. The clinical relevance of this finding can be observed in human CRC, in which the Bcl-xL protein expression as determined using immunohistochemistry was higher in KRAS-mutant tumors than in wild-type tumors (37). Notably, in the current study, Bcl-xL expression was further enhanced using a low dose (1-10 nM) of trametinib in all KRAS-mutant cells, significantly in G12D and G12V, in a dose-dependent manner. A similar trend was obtained from all KRAS mutants G12D, G12V and G13D. Among these mutants, G12V was selected for xenograft experiments because it produced the most stable and reproducible effects of trametinib with/or ABT263 on the proliferation (Figs. 3A, 4C and D).

The potential for Bcl-xL antagonism to increase apoptotic susceptibility during treatment with a MEK inhibitor in KRAS transductants was then investigated. ABT263 (1  $\mu$ M), a BH3 mimetic, synergistically enhanced trametinib (100 nM)-induced apoptosis in KRAS G12V transductants. Furthermore, it was identified that low-dose trametinib (10 nM) and ABT263 (10  $\mu$ M) synergistically induced apoptosis

more effectively in all KRAS-mutant transductants than in wild-type transductants. These results provide important insights regarding KRAS-mutant transduced cells as follows: i) Bcl-xL upregulation is considered a novel mechanism for KRAS-mediated resistance to apoptosis; ii) the interaction between trametinib and ABT263 synergistically promotes apoptosis; and iii) even at a low trametinib dose, a sufficient tumor-suppressive effect can be observed when combined with ABT263. Taken together, these data suggest that Bcl-xL upregulation is an important contributor to clinical resistance to MEK inhibitors in KRAS-mutant CRC.

The synergistic effect of low-dose trametinib and ABT263 on tumor suppression was supported by our Mix Culture Assay. This assay system is expected to be useful for screening the synergistic effects of multiple drugs targeting oncogene-mutant CRC.

For the murine *in vivo* xenograft model, KRAS G12V transductants were selected because of their stability. Tumorigenesis of the mutant cells was facilitated compared with the findings for wild-type cells, similar to the results of the *in vitro* experiments. The Bcl-xL and Bcl2 mRNA levels of the mutant xenografts were significantly higher than those of the wild-type xenografts, and this result was more noticeable than observed *in vitro*. This result is presumably because the expression of Bcl-xL and Bcl2 was further increased by resistance to cell death in mutant KRAS transductants when exposed to the stress of the *in vivo* environment because of immunity, cytokines, hypoxia, malnutrition and other variables. In the *in vivo* experiment examining combination therapy with trametinib and ABT263 in KRAS-mutant xenografts, xenograft growth was synergistically suppressed compared with effects of either agent alone. The doses used in this experiment were ~10-fold lower (0.1 mg/kg) for trametinib and ~20-fold lower (5 mg/kg) for ABT263 than reported previously (10,11,25,35). Trametinib has a number of side effects such as rash, diarrhea, fatigue and liver injury (38).

ABT263 has been reported to act selectively on cancer cells in a Bcl-xL-dependent manner, and combination treatment with ABT263 reduces the injury and inflammation induced in normal tissue by anticancer agents (39). Low-dose trametinib and ABT263 are expected to exert a synergistic effect and result in fewer adverse events in the treatment of KRAS-mutant CRC.

A limitation of the present study is that the difference in Bcl2 induction by KRAS mutations between CACO-2 and SW48 cells was not further investigated, and SW48 cells were not used for subsequent assays. CACO-2 cells were used in the mixed culture and apoptosis assays without SW48 cells for the following reasons. In the preliminary experiments, CACO-2 cells produced clearer results compared with SW48 cells. In addition, SW48 cells were considered as unusual CRC cells with mismatch repair deficiency. Because mismatch repair-deficient colorectal cancer is a rare type and exhibits different drug sensitivities compared with other CRC types, it was expected that using SW48 cells in these assays would likely not yield results consistent with clinical practice. On the other hand, CACO-2 cells are considered to be typical CRC cells with mismatch repair proficiency, TP53 mutation and APC mutation. Therefore, CACO-2 cells were used in subsequent experiments.



In conclusion, low-dose trametinib and ABT263 combination therapy targeting p-ERK and Bcl-xL, which are elevated by KRAS gene mutation, is expected to become a specific treatment modality for KRAS-mutant CRC.

### Acknowledgements

Not applicable.

### Funding

This study was supported by the Japan Society for the Promotion of Science KAKENHI (grant no. JP18K15238).

### Availability of data and materials

The datasets used and/or analyzed during the present study are available from the corresponding author on reasonable request.

### Authors' contributions

MKi, MT, SMiyag YS and TM contributed to the design of the study and editing of the manuscript. MKo, SN, SMiyaz, NH and TE performed the experiments, contributed to data analysis and wrote the manuscript. MT contributed to critical revision of the article. YM, FM, STō, MO, STa and YY participated in the experimental design, and interpreted the acquired data. All authors read and approved the final manuscript.

### Ethics approval and consent to participate

All animal experiments were carried out following the national standard of the care and use of laboratory animals, and the study was approved by the Animal Research Committee of Shinshu University (Matsumoto, Japan; approval no. 019046).

### Patient consent for publication

Not applicable.

### Competing interests

The authors declare that they have no competing interests.

### References

1. Stintzing S, Stremtizer S, Sebio A and Lenz HJ: Predictive and prognostic markers in the treatment of metastatic colorectal cancer (mCRC): Personalized medicine at work. *Hematol Oncol Clin North Am* 29: 43-60, 2015.
2. Adjei AA: Blocking oncogenic Ras signaling for cancer therapy. *J Natl Cancer Inst* 93: 1062-1074, 2001.
3. Yoon HH, Tougeron D, Shi Q, Alberts SR, Mahoney MR, Nelson GD, Nair SG, Thibodeau SN, Goldberg RM, Sargent DJ, *et al*: KRAS codon 12 and 13 mutations in relation to disease-free survival in BRAF wild-type stage III colon cancers from an adjuvant chemotherapy trial (N0147 alliance). *Clin Cancer Res* 20: 3033-3043, 2014.
4. Patricelli MP, Janes MR, Li LS, Hansen R, Peters U, Kessler LV, Chen Y, Kucharski JM, Feng J, Ely T, *et al*: Selective inhibition of oncogenic KRAS output with small molecules targeting the inactive state. *Cancer Discov* 6: 316-329, 2016.
5. Lito P, Solomon M, Li LS, Hansen R and Rosen N: Allele-specific inhibitors inactivate mutant KRAS G12C by a trapping mechanism. *Science* 35: 604-608, 2016.
6. Janes MR, Zhang J, Li LS, Hansen R, Peters U, Guo X, Chen Y, Babbar A, Firdaus SJ, Darjania L, *et al*: Targeting KRAS mutant cancers with a covalent G12C-specific inhibitor. *Cell* 172: 578-589.e17, 2018.
7. Garcia Fortanet J, Chen CH, *et al*: Allosteric inhibition of SHP2: Identification of a potent, selective, and orally efficacious phosphatase inhibitor. *J Med Chem* 59: 7773-7782, 2016.
8. Chen YN, LaMarche MJ, Chan HM, Fekkes P, Garcia-Fortanet J, Acker MG, Antonakos B, Chen CH, Chen Z, Cooke VG, *et al*: Allosteric inhibition of SHP2 phosphatase inhibits cancers driven by receptor tyrosine kinases. *Nature* 535: 148-52, 2016.
9. Lu H, Liu C, Velazquez R, Wang H, Dunkl LM, Kazic-Legueux M, Haberkorn A, Billy E, Manchado E, Brachmann SM, *et al*: SHP2 inhibition overcomes RTK-mediated pathway reactivation in KRAS-mutant tumors treated with MEK inhibitors. *Mol Cancer Ther* 18: 1323-1334, 2019.
10. Yamaguchi T, Kakefuda R, Tajima N, Sowa Y and Sakai T: Antitumor activities of JTP-74035(GSK1120212), a novel MEK1/2 inhibitor, on colorectal cancer cell lines *in vitro* and *in vivo*. *Int J Oncol* 39: 23-21, 2011.
11. Gilmartin AG, Bleam MR, Groy A, Moss KG, Minthorn EA, Kulkarni SG, Rominger CM, Erskine S, Fisher KE, Yang J, *et al*: GSK1120212(JTP-74057) is an inhibitor of MEK activity and activation with favorable pharmacologic properties for sustained *in vivo* pathway inhibition. *Clin Cancer Res* 17: 989-1000, 2011.
12. Roberts PJ and Der CJ: Targeting the Raf-MEK-ERK mitogen activated protein kinase cascade for the treatment of cancer. *Oncogene* 26: 3291-3310, 2007.
13. Kirkwood JM, Bastholt L, Robert C, Sosman J, Larkin J, Hersey P, Middleton M, Cantarini M, Zazulina V, Kemsley K and Dummer R: Phase II, open-label, randomized trial of the MEK1/2 inhibitor selumetinib as monotherapy versus temozolomide in patients with advanced melanoma. *Clin Cancer Res* 18: 555-567, 2012.
14. Adjei AA, Cohen RB, Franklin W, Morris C, Wilson D, Molina JR, Hanson LJ, Gore L, Chow L, Leong S, *et al*: Phase I pharmacokinetic and pharmacodynamics study of the oral, small-molecule mitogen-activated protein kinase kinase 1/2 inhibitor AZD6244 (ARRY-142886) in patients with advanced cancers. *J Clin Oncol* 26: 2139-2146, 2008.
15. Infante JR, Fecher LA, Nallapareddy S, Gordon MS, Flaherty KT, Cox DS, DeMarini DJ, Morris SR, Burris HA and Messersmith WA: Safety and efficacy results from the first-in-human study of the oral MEK 1/2 inhibitor GSK1120212. *J Clin Oncol* 28 (15\_Suppl): S2503, 2010.
16. Bennouna J, Lang I, Valladares-Ayerbes M, Boer K, Adenis A, Escudero P, Kim TY, Pover GM, Morris CD and Douillard JY: A phase II, open-label, randomised study to assess the efficacy and safety of the MEK1/2 inhibitor AZD6244 (ARRY-142886) versus capecitabine monotherapy in patients with colorectal cancer who have failed one or two prior chemotherapeutic regimens. *Invest New Drugs* 29: 1021-1028, 2011.
17. Zhao Y and Adjei AA: The clinical development of MEK inhibitors. *Nat Rev Clin Oncol* 11: 385-400, 2014.
18. Ascierto PA, Ferrucci PF, Fisher R, Del Vecchio M, Atkinson V, Schmidt H, Schachter J, Queirolo P, Long GV, Di Giacomo AM, *et al*: Dabrafenib, trametinib and pembrolizumab or placebo in BRAF-mutant melanoma. *Nat Med* 25: 941-946, 2019.
19. Tan N, Wong M, Nannini MA, Hong R, Lee LB, Price S, Williams K, Savy PP, Yue P, Sampath D, *et al*: Bcl-2/Bcl-xL inhibition increases the efficacy of MEK inhibition alone and in combination with PI3 kinase inhibition in lung and pancreatic tumor models. *Mol Cancer Ther* 12: 853-864, 2013.
20. Gong Y, Somwar R, Politi K, Balak M, Chmielecki J, Jiang X and Pao W: Induction of BIM is essential for apoptosis triggered by EGFR kinase inhibitors in mutant EGFR-dependent lung adenocarcinomas. *PLoS Med* 4: e294, 2007.
21. Hata AN, Yeo A, Faber AC, Lifshits E, Chen Z, Cheng KA, Walton Z, Sarosiek KA, Letai A, Heist RS, *et al*: Failure to induce apoptosis via BCL-2 family proteins underlies lack of efficacy of combined MEK and PI3K inhibitors for KRAS-mutant lung cancers. *Cancer Res* 74: 3146-3156, 2014.
22. Chen L, Willis SN, Wei A, Smith BJ, Fletcher JI, Hinds MG, Colman PM, Day CL, Adams JM and Huang DC: Differential targeting of prosurvival Bcl-2 proteins by their BH3-only ligands allows complementary apoptotic function. *Mol Cell* 17: 393-403, 2005.

23. Kawabata T, Tanimura S, Asai K, Kawasaki R, Matsumaru Y and Kohno M: Up-regulation of pro-apoptotic protein Bim and downregulation of anti-apoptotic protein Mcl-1 cooperatively mediate enhanced tumor cell death induced by the combination of ERK kinase (MEK) inhibitor and microtubule inhibitor. *J Biol Chem* 287: 10289-10300, 2012.
24. Meng J, Fang B, Liao Y, Chresta CM, Smith PD and Roth JA: Apoptosis induction by MEK inhibition in human lung cancer cells is mediated by Bim. *PLoS One* 5: e13026, 2010.
25. Corcoran RM, Cheng KA, Hata AN, Faber AC, Ebi H, Coffee EM, Greninger P, Brown RD, Godfrey JT, Cohoon TJ, *et al*: Synthetic lethal interaction combined BCL-XL and MEK inhibition promotes tumor regressions in KRAS mutant cancer models. *Cancer Cell* 14: 121-128, 2013.
26. Scherr AL, Gdynia G, Salou M, Radhakrishnan P, Duglova K, Heller A, Keim S, Kautz N, Jassowicz A, Elssner C, *et al*: Bcl-xl is an oncogenic driver in colorectal cancer. *Cell Death Dis* 7: e2342, 2016.
27. Zaanani A, Okamoto K, Kawakami H, Khazaie K, Huang S and Sinicrope FA: Mutant KRAS upregulates BCL-XL via STAT3 to confer apoptosis resistance that is reversed by BIM induction and BCL-XL antagonism. *J Biol Chem* 290: 23838-23849, 2015.
28. Kitazawa M, Hida S, Fujii C, Taniguchi S, Ito K, Matsumura T, Okada N, Sakaizawa T, Kobayashi A, Takeoka M and Miyagawa SI: ASC induces apoptosis via activation of caspase-9 by enhancing gap junction-mediated intercellular communication. *PLoS One* 12: e0169340, 2017.
29. Livak KJ and Schmittgen TD: Analysis of relative gene expression data using real time quantitative PCR and the 2(Delta Delta C(T)) method. *Methods* 25: 402-408, 2001.
30. Jonker DJ, O'Callaghan CJ, Karapetis CS, Zalcberg JR, Tu D, Au HJ, Berry SR, Krahn M, Price T, Simes RJ, *et al*: Cetuximab for the treatment of colorectal cancer. *N Engl J Med* 357: 2040-2048, 2007.
31. Van Cutsem E, Köhne CH, Hitre E, Zaluski J, Chang Chien CR, Makhson A, D'Haens G, Pintér T, Lim R, Bodoky G, *et al*: Cetuximab and chemotherapy as initial treatment for metastatic colorectal cancer. *N Engl J Med* 360: 1408-1417, 2009.
32. Amado RG, Wolf M, Peeters M, Van Cutsem E, Siena S, Freeman DJ, Juan T, Soikorski R, Suggs S, Radinsky R, *et al*: Wild-type KRAS is required for panitumumab efficacy in patients with metastatic colorectal cancer. *J Clin Oncol* 26: 1626-1634, 2008.
33. Karapetis CS, Khambata-Ford S, Jonker DJ, *et al*: K-ras mutations and benefit from cetuximab in advanced colorectal cancer. *N Engl J Med* 359: 1757-1765, 2008.
34. Douillard JY, Oliner KS, Siena S, Tabernero J, Burkes R, Barugel M, Humblet Y, Bodoky G, Cunningham D, Jassem J, *et al*: Panitumumab-FOLFOX4 treatment and RAS mutations in colorectal cancer. *N Engl J Med* 369: 1023-1034, 2013.
35. Cho SY, Han JY, Na D, Kang W, Lee A, Kim J, Lee J, Min S, Kang J, Chae J, *et al*: A novel combination treatment targeting BCL-XL and MCL1 for KRAS/BRAF-mutated and BCL2L1-amplified colorectal cancers. *Mol Cancer Ther* 16: 2178-2190, 2017.
36. Ahmed D, Eide PW, Eilertsen IA, Danielsen SA, Eknæs M, Hektoen M, Lind GE and Lothe RA: Epigenetic and genetic features of 24 colon cancer cell lines. *Oncogenesis* 16: e71, 2013.
37. Kasper S, Breitenbuecher F, Reis H, Brandau S, Worm K, Köhler J, Paul A, Trarbach T, Schmid K and Schuler M: Oncogenic RAS simultaneously protects against anti-EGFR antibody-dependent cellular cytotoxicity and EGFR signaling blockade. *Oncogene* 32: 2873-2881, 2013.
38. Welsh SJ and Corrie PG: Management of BRAF and MEK inhibitor toxicities in patients with metastatic melanoma. *Ther Adv Med Oncol* 7: 122-1236, 2015.
39. Tutusaus A, Stefanovic M, Boix L, *et al*: Antiapoptotic BCL-2 proteins determine Sorafenib/regorafenib resistance and BH3-mimetic efficacy in hepatocellular carcinoma. *Oncotarget* 30: 16701-16717, 2018.